Meteorologische Zeitschrift, Vol. **18**, No. 6, 647-661 (December 2009)

Article

The residual of the energy balance closure and its influence on the results of three SVAT models

DANIELA KRACHER*[1,2], HEINZ-THEO MENGELKAMP[3] and THOMAS FOKEN[1]

[1]Department of Micrometeorology, University of Bayreuth, Germany
[2]Current affiliation: Karlsruhe Institute of Technology, Institute for Meteorology and Climate Research IMK-IFU, Garmisch-Partenkirchen, Germany
[3]Institute for Coastal Research, GKSS Research Centre, Geesthacht, Germany

(Manuscript received December 9, 2008; in revised form April 14, 2009; accepted August 10, 2009)

Abstract

Commonly used measuring methods only allow for a closure of the energy balance at the Earth's surface except for a residual. Models, in contrast, inherently demand an entirely closed energy balance, which they achieve in different ways. This paper examines the model simulations depending on the methods used for closing the energy balance, the optimization of the parameters, and the equations used. The one-dimensional surface vegetation atmosphere transfer (SVAT) models REMO, SEWAB and TERRA, which were made available by the GKSS Institute in Geesthacht, are examined and compared with measured data from the LITFASS-2003 experiment. LITFASS-2003 took place during May and June 2003 in the experimental fields of the Meteorological Observatory Lindenberg. Parameter sets optimized with regard to the turbulent fluxes yield better results, but are often not consistent with site characteristics and differ within the models. We ran the models with the optimized parameter sets, and with a set of selected parameters which agree with the respective sites. SEWAB closes the energy balance by using an iteration of the surface temperature, through which the influence of the residual is distributed over all fluxes. In REMO and TERRA the soil heat flux is estimated as the residual of the other components of the energy balance equation. This results in an extreme overestimation of this heat flux. Parameter optimization has an impact on the partitioning of the available energy and its distribution to the turbulent heat fluxes. It does not influence the effect of the residual on the results. Currently we do not know how to close the measured energy balance at the surface appropriately because of the underestimation of the turbulent fluxes by eddy-covariance measurements and the unknown partitioning of the residual between the sensible and latent heat flux. Therefore, the method used in SEWAB yields better results than the one used in REMO and TERRA. The method used to close the energy balance has more impact on the simulated surface energy balance components than does their parameterization. For this reason it is not possible to attribute the differences in the calculated heat fluxes to particular differences in the equations and parameters.

Zusammenfassung

Gewöhnlich sind unsere Messmethoden nur in der Lage, die Energiebilanz an der Erdoberfläche bis auf ein Residuum zu schließen. Modelle erfordern dagegen eine interne Schließung der Energiebilanz, welche auf verschiedene Weise erfolgen kann. In diesem Artikel wird das Energiebilanz-Schließungsproblem in Modellsimulationen untersucht in Abhängigkeit von der Schließungsmethode, der Optimierung der Parameter und der angewandten Gleichungen. Die eindimensionalen SVAT-Schemata der Modelle REMO, SEWAB und TERRA, welche durch das GKSS Institut in Geesthacht zur Verfügung gestellt wurden, wurden genutzt und verglichen mit Messdaten des LITFASS-2003 Experiment. LITFASS-2003 fand im Mai und Juni 2003 auf Messflächen des Meteorologischen Observatoriums Lindenberg statt. Die anhand der turbulenten Flüsse optimierten Parameter der drei Modelle sind oft nicht konsistent mit den Messflächeneigenschaften und unterscheiden sich für die verschiedenen Modelle. Die Modellrechnungen wurden daher mit den optimierten Parametersätzen und mit einem Satz ausgewählter Parameter, die mit den Messflächen übereinstimmen, durchgeführt. SEWAB schließt die Energiebilanz durch eine iterative Bestimmung der Oberflächentemperatur, womit der Einfluss des Residuums auf alle Flüsse verteilt wird. In REMO und TERRA wird der Bodenwärmestrom als Restglied aus allen anderen Komponenten der Energiebilanzgleichung bestimmt. Daraus folgt eine extreme Überbestimmung dieses Wärmestroms. Die Parameteroptimierung hat Einfluss auf die Verteilung der verfügbaren Energie auf die turbulenten Wärmeflüsse, beeinflusst aber nicht den Effekt des Residuums auf die Ergebnisse. Aufgrund der Unterbestimmung der turbulenten Wärmeflüsse mit der Eddy-Kovarianz Messungen und der bisher unbekannten Zusammensetzung des Residuums aus fühlbarem und latentem Wärmestrom wird die in SEWAB verwendete Methode als besser angesehen als die Methodik in TERRA und REMO. Die Methode der Schließung der Energiebilanz hat einen größeren Einfluss auf die simulierten Energiebilanzkomponenten als ihre Parametrisierung. Dadurch ist es nicht möglich die Unterschiede bei den Wärmeflüssen speziellen Unterschieden in den Gleichungen und Parametersätzen zuzuordnen.

*Corresponding author: Daniela Kracher, Karlsruhe Institute of Technology, IMK-IFU, 82467 Garmisch-Partenkirchen, e-mail: daniela.kracher@imk.fzk.de

DOI 10.1127/0941-2948/2009/0412
0941-2948/2009/0412 $ 6.75

1 Introduction

From experiments in the 1970s and 1980s ELAGINA et al. (1973), ORLENKO and LEGOTINA (1973), KOITZSCH et al. (1988) and others found that the energy balance was not closed by the measured components. They attributed the apparent residual to measurement errors and did not consider other explanations. In the 1990s the focus went back to the unclosed energy balance (FOKEN, 1990; TSVANG et al., 1991, DUGAS et al., 1991; FOKEN and ONCLEY, 1995). In almost all experiments where the energy balance equation could not be closed, the net radiation was higher than the sum of the other components of the energy balance equation. The energy balance for the surface can be written as

$$-Q{*}_S = Q_H + Q_E + Q_G \qquad (1.1)$$

where $Q{*}_S$ is the net radiation, Q_H the sensible heat flux, Q_E the latent heat flux and Q_G the soil heat flux. At present, an unclosed energy balance is found for most of the experiments with a residual of 10–30 % of the net radiation (LAUBACH and TEICHMANN, 1996; FOKEN, 1998; AUBINET et al., 2000; WILSON et al., 2002; CULF et al., 2004) which can be included in Equation (1) as the additional term "residual". Recently turbulent organized structures and secondary circulations are assumed to be a main factor of the phenomena (KANDA et al., 2004; INAGAKI et al., 2006; FOKEN, 2008; STEINFELD et al., 2007; MAUDER et al., 2007a).

Most processes taking place at the surface are dependent on the available energy in a direct or indirect way. Therefore the energy balance equation is a crucial part of Surface-Vegetation-Atmosphere-Transfer (SVAT) models to simulate exchange processes at the surface. As models need to be tested against measurements, a potential deficiency in the measured energy balance equation needs to be taken into account in order to guarantee both a closed energy balance equation within the model and a reasonable calculation of the surface energy fluxes. In this study we examine the different methods used in the models to ensure a closed energy balance, and analyse the effects on the simulated components of the energy balance equation.

For accurately calculating the exchange of energy, water and gases at the surface, SVAT models need a large number of parameters which represent the environmental conditions. Usually more complex models demand a significant higher number of parameters than simpler models in order to achieve accurate simulations. But on the other hand, models with fewer parameters are much more easily used for different sites than are complex models. For example the SiSPAT model (Simple Soil Plant Atmosphere Transfer, BRAUD et al., 1995) needs about 60 parameters, which are difficult to estimate for each plot. The ISBA model (Interactions Soil Biosphere Atmosphere, NOILHAN and MAHFOUF, 1996) however, which is used by the French weather service, needs only 10 parameters and can therefore be applied more easily. For most models, the parameters need to be optimized to adapt the models to the respective site (SCHAAKE, 2003). Sometimes models lack accuracy in parts of some of their equations for one or more possible reasons: because the main focus lies on other parts of the model, the described processes are not yet fully understood, the intention was to keep the calculations more simple, or because the calculations rely on specific assumptions and might not be applicable in the same form for different situations. In any case, a parameter optimization is a good tool to compensate for such model deficiencies. Ideally the parameters are optimized within the most probable range for the respective site. That implies the requirement of an adequate measurement data base, which is most often not available. Consequently the parameters are optimized within a wide range, so that a realistic representation of site specific properties might not be given. Therefore we ran the models with optimized and site representative parameters to examine how an optimization influences the residual's effect in the simulations.

2 Experimental basis: The LITFASS-2003 experiment

This study is based on the data of the LITFASS-2003 experiment (BEYRICH et al., 2006; BEYRICH and MENGELKAMP, 2006) which was carried out from 19th of May 2003 to 17th of June 2003 in the landscape around the Meteorological Observatory Lindenberg (MOL) of the German Weather Service south-east of Berlin, Germany. Basic atmospheric parameters such as air temperature, air humidity, wind speed and wind direction as well as the major components of the surface energy budget (net radiation, sensible heat flux, latent heat flux and soil heat flux) were measured at 14 micrometeorological stations over different vegetation types. As part of the operational measurement programme of the MOL, four of them are operated over a long-term period. The other 10 stations were set up especially for the period of the experiment and placed at agricultural fields with crops that are typical for that region (cereals, particularly rye and triticale, rape and maize). To ensure identical data processing, all measurements were analysed with the same software package (MAUDER et al., 2006). For this experiment, comprehensive investigations of the energy balance closure are available with an error analysis of all measurements (MAUDER et al., 2006), special investigations of the eddy covariance measurements (MAUDER and FOKEN, 2006), the influence of long wave turbulent fluxes (FOKEN et al., 2006) as well as an overview with conclusions (FOKEN et al., 2009). For our study we used the eddy covariance data from two agricultural sites, a rye field and a maize field, which were separated by a farm track. All data were averaged for equal time intervals of 30 minutes over a time period with all measured flux data available. These averaged data were used to calculate the mean daily cycles of the energy fluxes so that a better comparison of the data and clarification of tendencies was achieved.

3 Model description

For our investigation we used the three 1D SVAT-models REMO, SEWAB and TERRA. REMO (REgional MOdell) is the 'stand alone' version of the climate model REMO (JACOB and PODZUN, 1997), SEWAB (Surface Energy WAter Balance) is used at the GKSS Institute in Geesthacht for hydrological simulations (MENGELKAMP et al., 1999; 2002; WARRACH et al., 2002) and TERRA is part of the LM (Lokal Modell) of the German Weather Service (DWD, 1995[1]; STEPPELER et al., 2003). At the GKSS Institute 1D standalone versions from the TERRA and REMO model were extracted and provided for this study. Therefore the program codes are not necessarily identical to the original models. For abbreviations and symbols used, see section 6.

3.1 Equations

SEWAB and TERRA calculate the energy fluxes with a bulk approach:

$$Q_H = \rho \cdot c_p \cdot C_H \cdot u(z) \cdot (\Theta(z) - \Theta_0) \quad (3.1)$$

$$Q_E = \rho \cdot \lambda \cdot C_E \cdot u(z) \cdot (q(z) - q_0) \quad (3.2)$$

where ρ is the air density, c_p the specific heat of air at constant pressure, λ the heat of evaporation, u the wind velocity, Θ the potential temperature, q the specific air humidity and C_H is the Stanton number. The Dalton number C_E is the equivalent for water vapor. Taking into account stratified conditions, LOUIS (1979) inserted a correction term F_h that is dependent on the Bulk Richardson number Ri_B and the roughness length z_0

$$C_H = C_{hn} \cdot F_h(Ri_B, z/z_0) \quad (3.3)$$

where C_{hn} is the transfer coefficient for heat for neutral conditions considering the roughness length for temperature, z_{0T}:

$$C_{hn} = \frac{\kappa}{\ln\left(\frac{z}{z_0}\right) \ln\left(\frac{z}{z_{0T}}\right)} \quad (3.4)$$

SEWAB uses the correction terms after LOUIS (1979), and TERRA the modified ones after LOUIS et al. (1982) (see Table 1). REMO also shows similarity to the bulk approach in the calculation of the sensible heat flux

$$Q_H = \frac{1{,}5 \cdot \frac{1}{R_L} \cdot p \cdot u}{(T_V - T \cdot C_W)\left(1 + 10 \cdot Ri \cdot \sqrt{1 + |Ri_B|}\right)} \cdot C_{hn} \cdot \left(ZTDIF - 1/3 \cdot \Theta - T \cdot c_p\right) \quad (3.5)$$

as well as the latent heat flux

$$Q_E = \lambda \cdot \frac{\frac{1}{R_L} \cdot p \cdot u}{(T_V - T \cdot C_W)\left(1 + 10 \cdot Ri_B \cdot \sqrt{1 + |Ri_B|}\right)} \cdot C_{hn} \cdot (q - r \cdot q_{sat}) \quad (3.6)$$

where T_v is the virtual temperature, C_W the water content of clouds, R_L the gas constant for dry air and r the relative humidity. ZTDIF represents an artifact of a recursive method that is not documented further in the program code and that is only used for the sensible heat flux, but not for the latent heat flux. Hence, it is only of importance for the original REMO model used for regional simulations, and not for the 1D standalone version we are using for this study. Even though REMO shows similarities to the bulk approach, there already are, in the main equations for the sensible and latent heat fluxes, distinct differences from the calculations used in SEWAB and TERRA, which themselves are quite similar in their main equations. When considered in more detail, SEWAB and TERRA also show more differences in their calculations, see Table 1.

In REMO the net radiation is calculated without taking into account the reflected shortwave radiation:

$$ZNET = K \downarrow + \varepsilon_{eff} \cdot \sigma \cdot T^4 \quad (3.7)$$

where $K\downarrow$ is the global radiation, σ the Stefan-Boltzmann-constant and ε_{eff} an effective emissivity, which represents an already balanced long wave radiation. In this study we focus on the effect of the energy balance closure problem on the model outcome. The net radiation is crucial for investigations concerning the energy balance at the surface, and a wrong calculation may lead to wrong conclusions regarding the effect of the residual on the simulated fluxes. Therefore we implemented an equation for the net radiation that includes the reflected shortwave radiation $K\uparrow$ in order to enable a more realistic calculation:

$$ZNET = K \downarrow + K \uparrow + \varepsilon_{eff} \cdot \sigma \cdot T^4 \quad (3.8)$$

The optimized albedo value that was already available in REMO was not appropriate due to the incomplete equation for the net radiation, so that for our newly implemented equation we used a more realistic albedo value of 0.2. We are aware that we are thereby simulating a net radiation that was not originally present in this form in the program code.

SEWAB calculates the soil heat flux from the soil heat conductivity λ_{soil} and the temperature difference

[1] Documentation of the EM/DM-System, Version 1.0

Table 1: Comparison of the equations used in SEWAB and TERRA, see section 6 for an explanation of the symbols.

	SEWAB	TERRA
$Ri_B > 0$:	$F_h = \frac{1}{(1+4{,}7 Ri_B)^2}$	$F_h = \frac{1}{1+15 \cdot Ri_B \cdot \sqrt{1+5 \cdot Ri_B}}$
$Ri_B < 0$:	$F_h = 1 - \frac{9{,}4 \cdot Ri_B}{1+9{,}4 \cdot C_{hn} \cdot 5{,}3 \cdot \sqrt{\frac{z}{z_0} \cdot \lvert Ri_B \rvert}}$	$F_h = 1 - \frac{15 \cdot Ri_B}{1+75 \cdot C_{hn}\left[\left(\frac{z}{z_{0T}}\right)^{\frac{1}{3}} - 1\right]^{\frac{3}{2}} \cdot \sqrt{\lvert Ri_B \rvert}}$
	$C_{hn} = \frac{\kappa?}{\ln\left(\frac{z}{z_0}\right)\left[\ln\left(\frac{z}{z_0}\right) + 2{,}3\right]}$	$C_{hn} = \frac{\kappa?}{\left[\ln\left(\frac{z}{z_0}\right)\right]^2} = C_{mn}$
	$Q^*_S = K_{netto} - L\downarrow + \varepsilon \cdot \sigma \cdot T_0^4$	$Q^*_S = K_{netto} - L\downarrow + \varepsilon \cdot \sigma \cdot T_0^4$
	$ET_B = \rho_W \cdot u \cdot C_{hn} \cdot F_h \cdot (R_B \cdot q_{sat,0} - q)$	$ET_B = \rho_W \cdot C_h (q_{sat,0} - q) = EP$
	$ET_{Int} = \delta_I \cdot u \cdot C_{hn} \cdot F_h \cdot (q_{sat,0} - q)$	$ET_{Int} = \delta_I \cdot u \cdot C_{hn} \cdot F_h \cdot (q_{sat,0} - q)$
	$ET_V = \frac{1}{r_a + r_s} \cdot \rho_W \cdot (q_{sat,0} - q)$	$ET_V = (1-\delta_I) \cdot \frac{EP \cdot \frac{LAI}{r_a + r_s}}{\frac{LAI}{r_a + r_s} + C_H}$
	$K_{netto} = -K\downarrow \cdot (1 - (\delta_V \cdot a_V + (1-\delta_V) \cdot a_B) \cdot HH1)$	$K_{netto} = (1-a) \cdot K\downarrow$
	$HH1 = 0{,}085 + \frac{1}{1+10 \cdot \cos\Psi}$	
	$\lambda_{soil} = -\frac{(1-\eta_{sat}) \cdot 25 + \eta \cdot 0{,}56 + \left(\eta_{sat} - \eta - \eta_I \cdot \frac{\rho_I}{\rho_W}\right) \cdot 0{,}025 + \eta_I \cdot 2{,}26}{-0{,}1}$	

between the surface T_0 and the upper soil layers T_S:

$$Q_G = \lambda_{soil} \cdot (T_0 - T_S) \tag{3.9}$$

In REMO and TERRA there is no such explicit calculation for the soil heat flux. TERRA balances the soil heat flux with the other components of the energy balance equation and simultaneously closes the energy balance. In REMO there was originally no equation available regarding the soil heat flux. As the energy balance is closed by definition, we also assumed for our version of the REMO model that the energy balance is closed. Without changing other calculations, the only option left was to calculate the soil heat flux the same way as it is done in TERRA.

With our changes in the program code, the 1D standalone version of REMO we were using for our study differs even more from the original REMO model. However, we will refer to our version as "REMO", even though we are aware that there are differences to the original model.

3.2 Parameters

All three models need identical forcing time series of date, time, precipitation, air temperature, wind velocity, air pressure, relative humidity, global radiation, and incoming long wave radiation. In our case we used measurements obtained during the LITFASS-2003 experiment.

Each model has a number of parameters to represent soil, vegetation and atmospheric properties. These parameters were optimized with respect to the measured latent and sensible heat fluxes. All optimized parameter sets were provided by the GKSS Institute in Geesthacht. An exemplary description of the optimization for TERRA is given in JOHNSEN et al. (2006).

An overview of all the parameters that were optimized for the three models is presented in Table 2. Only 6 parameters were optimized for all three models (roughness length, albedo, emissivity, field capacity, soil heat capacity and minimal stomatal resistance). The parameters included in the optimization are different for the three models, because the models differ in their equations and in their sensitivity on specific parameters.

Table 2: Overview of the optimized parameters.

	SEWAB	TERRA	REMO
Albedo	x	x	x
Canopy height	x		
Exponent b	x		
Heat capacity (volumetric)	x	x	x
Constant for interception storage (dewatering)		x	
Constant for maximal interception storage		x	
Fraction of photosynthetic active radiation		x	x
Factor to calculate stomatal resistance	x		
Correction factor for field capacity			x
Factor for heat conductivity of the soil			x
Saturated hydraulic conductivity	x		
Leaf area index	x	x	x
Maximal stomatal resistance		x	
Minimal stomatal resistance	x		x
Pore volume		x	x
Rooting depth	x	x	
Correction factor for soil temperature		x	
Roughness length	x	x	x
Fraction of area covered by vegetation		x	x
Emissivity	x	x	x
Effective emissivity			x
Field capacity	x	x	x
Volumetric water content at saturation	x		
Volumetric water content at wilting point	x		
Soil heat conductivity	x		
Heat conductivity of dry soil			x
Matric potential at saturation	x		

In the optimization process the model is run with many different parameter sets to define the parameter set which leads to the best simulations. The parameter sets are created by changing the value of each parameter included in the optimization process within a given range. For the optimization of REMO, SEWAB, and TERRA, a SCE-UA (Shuffled Complex Evolution – University of Arizona) algorithm (Duan et al., 1992; Duan et al., 1994) was used followed by a MOSCEM-UA (Multiobjective Shuffled Complex Evolution Metropolis – University of Arizona) algorithm (Vrugt et al., 2003), both being developed for hydrological models. The SCE-UA algorithm defined the global optimum in the parameter space of each model for the parameters listed in Table 2. With the MOSCEM-UA algorithm a multi-objective optimization of a selection of parameters identical for all three models was conducted afterwards. A more detailed overview is given in Table 3, which shows all parameters that are optimized for at least two models plus the parameters used in SEWAB to calculate the soil heat flux. As SEWAB is the only model calculating the soil heat flux explicitly, the parameters needed for the calculations are not used in TERRA and REMO.

Although the parameters are optimized for the same sites, there are distinct differences in the values of especially the leaf area index, the heat capacity and the field capacity. The albedo optimized for SEWAB and TERRA is quite similar, whereas the original values optimized

Table 3: Selection of optimized parameters and parameters chosen as realistic, in comparison for both sites.

	Maize				Rye			
	REMO	**SEWAB**	**TERRA**	**realistic**	**REMO**	**SEWAB**	**TERRA**	**realistic**
z_0	0.0101	0.0100	0.0104	0.044	0.013	0.0121	0.0134	0.179
LAI	4.7	–	3.7	1.5	2.92	3.81	2.94	2.73
A	0.2(0.5)	0.25	0.24	0.2	0.2(0.5)	0.21	0.41	0.18
ε	0.996	0.979	0.914	0.986	0.996	0.967	0.997	0.986
η_{fc}	0.773	0.184	0.139	0.342	0.166	0.392	0.126	0.342
$c_{soil} \cdot \rho_{soil}$	$5.84 \cdot 10^5$	$4.90 \cdot 10^6$	$1.79 \cdot 10^6$	$1.8 \cdot 10^6$	$5.66 \cdot 10^5$	$4.52 \cdot 10^6$	$1.04 \cdot 10^6$	$1.8 \cdot 10^6$
z_r	–	0.30–0.50	0.514	0.25	–	0.10–0.30	0.509	0.6
f_{PAR}	–	–	0.463	0.5	–	–	0.463	0.5
V_{por}	0.338	–	0.368	0.43	0.470	–	0.532	0.43
$r_{s.min}$[1]	100	487.898	60	60	100	144.24	60	300
$r_{s.max}$[2]	–	2500	20.642	2500	–	2500	22.290	2500
δ_V	0.509	–	0.689	0.7	0.507	--	0.757	1
z_c	–	0.60	–	0.45	–	0.60	–	1.2
η_{sat}	–	0.349	–	0.44	–	0.591	–	0.44
ψ_{sat}	--	-0.515	–	-0.1	–	-0.437	–	-0.1
K_{sat}	–	$2.52 \cdot 10^{-4}$	–	$5.23 \cdot 10^{-6}$	–	$6.13 \cdot 10^{-5}$	–	$5.23 \cdot 10^{-6}$
η_{WP}	–	0.115	–	0.15	–	0.259	–	0.15
b	–	11.21	–	4.80	–	8.09	–	4.80

[1] set constant, but not optimized for REMO and TERRA
[2] set constant, but not optimized for SEWAB

for REMO were too high (0.5 – for land surface) due to the incomplete calculation of the net radiation. As we had to include a new equation for the net radiation, we simultaneously set the albedo to a new value of 0.2 to ensure a realistic calculation. In REMO, only the minimal stomatal resistance is used for the calculations and is set constant to 100 s m^{-1}. TERRA optimizes the minimal stomatal resistance and sets the maximal stomatal resistance equal to 60 s m^{-1}, which is lower than the maximal stomatal resistance in REMO and much lower than the maximal stomatal resistance in SEWAB (2500 s m^{-1}). The stomatal resistance is calculated in SEWAB according to NOILHAN and PLANTON (1989) and the minimal stomatal resistance is optimized. The values of the constants are not further explained or documented in the program codes, so that the differences between the minimal and maximal stomatal resistances cannot be explained. The root depth in SEWAB is not given as a length, but as the respective soil layer.

Most parameters were optimized to different values for the three models. This shows that the parameter optimization compensates, as already mentioned earlier, for model deficiencies at the cost of a realistic representation of site specific properties. It should be an aim of modelling to gain proper results with the most realistic parameters so that an optimization is only needed for non-measurable or non-available parameters. Going from one-dimensional to regional simulations, where single parameters represent a model grid cell, this problem becomes even more important.

With the optimized parameters, we compared the models at a stage where they are close to their best performance. To see whether an optimization influences the effect of the residual on the model outcome, we also ran the models with a set of non-optimized parameters. To this end, we defined a set of parameters for which we tried to find the most realistic values. In doing so we chose parameters that are used in at least 2 models and

Table 4: Volumetric heat capacities for different soil water contents (ALTMAN and DITTMER (1966).

volumetric water content $m^3\ m^{-3}$	heat capacity 10^6 J m^{-3} K^{-1}
0	1.26 – 1.67
0.2	1.67 – 2.5
0.4	2.5 – 3.3

Table 5: Literature values for saturated hydraulic conductivity; the value from AG Boden (1994) was averaged from different values given for a range of bulk densities.

Literature	K_{sat} [m s^{-1}]
HARTGE und HORN (1999)	$4{\cdot}10^{-3}$ - $1{\cdot}10^{-9}$
NOVAK et al. (2005)	$5.62{\cdot}10^{-7}$
AG BODEN (1994)	$1.2346{\cdot}10^{-6}$
COSBY et al. (1984)	$5.23{\cdot}10^{-6}$
LI et al. (1976)	$3.47{\cdot}10^{-5}$

a set of soil specific parameters used only in SEWAB, summarized in Table 3.

Some of the parameters we selected for the set of realistic parameters, namely roughness length, leaf area index and albedo, were already estimated during the LITFASS-2003 experiment (BEYRICH et al., 2006). For the rye field, roughness length, leaf area index and albedo were measured to 0.179, 2.7 and 0.18, respectively. The roughness length for the maize field was measured to 0.044, the albedo to 0.2, while the leaf area index was not measured, but estimated to be 1.5. For both fields the emissivity is set to 0.986, following GEIGER et al. (1995). The field capacity for sandy loam was calculated as a mean value of 0.34 from the values for different bulk densities given in AG Boden (1994). The heat capacity is the product of specific heat and density of the soil. HARTGE and HORN (1999), gives different volumetric heat capacities for different water contents; see Table 4. As the soil was dry during the experiment and as the heat capacities of the soil components such as clay minerals, humus, and water are higher than the interval for dry soil (SCHEFFER and SCHACHTSCHABEL, 2002), we chose $1.7 \cdot 10^6$ J m^{-3} K^{-1} as a realistic value. The root depth was estimated for both sites, namely 20 cm for the maize field and 60 cm for the rye field. Following LARCHER (1994), the photosynthetic active radiation contributes 45 to 50 % of the global radiation. As the fraction can be even larger, we used 50 % for our realistic parameter selection. The pore volume for loam is set to 43 %, which is the mean between 30 % and 55 % as given by SCHEFFER and SCHACHTSCHABEL (2002). For the minimal stomatal resistance of maize MONTEITH (1976) gives a value of 40 s m-1, whereas in SELLERS (1985) and GOTTSCHALCK et al. (2001) values of 50 s m^{-1} and 79 s m^{-1} respectively can be found. We decided to choose a mean value of 60 s m^{-1} for our set of realistic parameters. For the rye field we took the value for wheat proposed by ALTMAN and DITTMER (1966), 300 s m^{-1}. As the rye field was totally covered by crops a value of 1 is appropriate for the fraction of plant covered area. The maize plants were growing during the experiment, but the area between the maize plants was covered by weeds so that we chose a value of 0.7. The mean of the canopy height was estimated as 0.45 m for the maize field and 1.2 m for the rye field. For the saturated hydraulic conductivity there are different values given in the literature; see Table 5. We chose $5.23{\cdot}10^{-6}$ (COSBY et al., 1984) as a representative value. The matrix potential at saturation for sandy loam was estimated in COSBY et al. (1984) as –0.141 and in CLAPP and HORNBERGER (1978) as –0.072. For our simulations we chose a value of –0.1. According to a figure in SCHROEDER (1992) the water content at wilting point was set to 0.15. The gradient of the logarithmic retention curve (exponent b) was estimated by CLAPP and HORNBERGER (1978) as 4.9 and by COSBY et al. (1984) as 4.74 for sandy loam. For our set of realistic parameters we set the exponent b to 4.8. The volumetric water content at saturation is given in SCHEFFER and SCHACHTSCHABEL (2002) as 0.45 (as read from a graph). COSBY et al. (1984) and CLAPP and HORNBERGER (1978) suggest a value of 0.434 and 0.435, respectively. Considering this, we chose 0.44.

4 Results and discussion

To get an impression of the coherence between the residual and the results, the differences between simulated and measured surface fluxes were plotted versus the residual from the measured energy balance equation. To this end, we subtracted the modelled values from the measured values. This is indicated exemplary as Q_H (UBT-R), where UBT means measured values from the University of Bayreuth and R is an abbreviation for REMO and is replaced by S for SEWAB and T for TERRA. Consequently, positive values show underestimated and negative values overestimated fluxes. As the net radiation is negative by definition, here it is the other way round, which means that a positive difference shows an overestimation and vice versa. We made this comparison for both the optimized and the realistic parameters.

For most cases, the differences between measured and simulated fluxes are much higher during the day than during the night. The curve of the residual shows a maximum value around noon, which can clearly be seen for

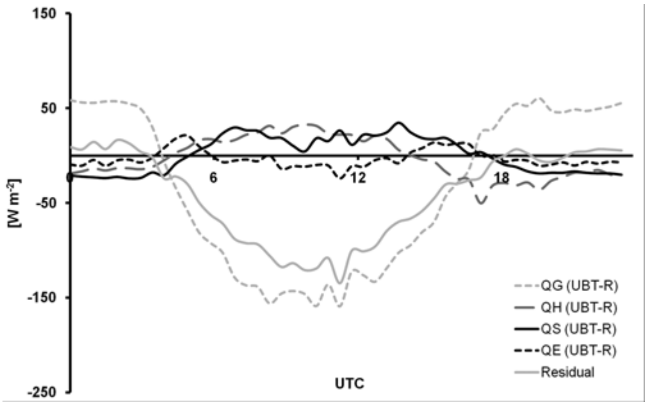

Figure 1: Differences between the energy fluxes simulated with REMO (optimized parameters) for the maize field and the measured values, versus time of day. Also shown is the residual in the measured energy balance.

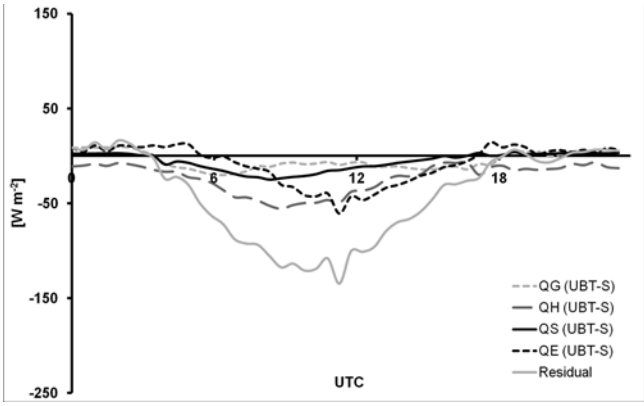

Figure 3: Differences between the energy fluxes simulated with SEWAB (optimized parameters) for the maize field and the measured values, versus time of day. Also shown is the residual in the measured energy balance.

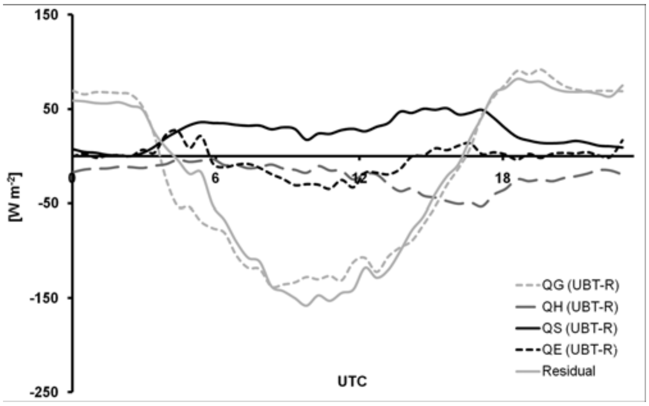

Figure 2: Differences between the energy fluxes simulated with REMO (optimized parameters) for the rye field and the measured values, versus time of day. Also shown is the residual in the measured energy balance.

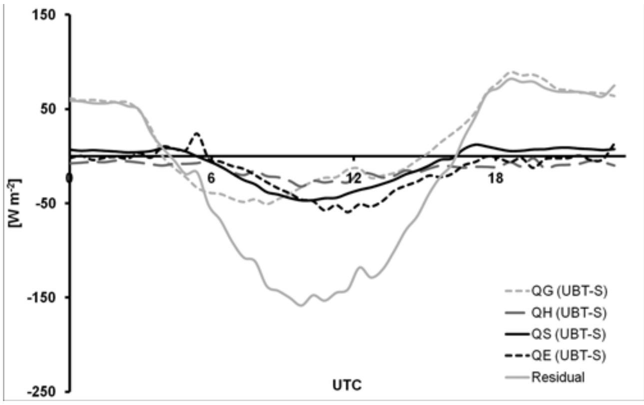

Figure 4: Differences between the energy fluxes simulated with SEWAB (optimized parameters) for the rye field and the measured values, versus time of day. Also shown is the residual in the measured energy balance.

both fields. But the night pattern for the residual differs between the rye and the maize field. At the maize field the residual is almost zero during the night (Figure 1) whereas at the rye field it is up to 50 W m^{-2} (Figure 2).

This high residual during night implies that there are uncertainties in the measurement quality for the rye field, which might be due to the measurement equipment. However, especially for the maize field, the measurement equipment was of high quality and a special focus was on the measurement of the soil heat flux. As the non-closure of the energy balance by measurements is due to a problem concerning the turbulent fluxes, the residual should be zero during night, when the turbulent fluxes are also around zero.

Simulations with optimized parameters

In the simulation with the optimized parameters, REMO (Figures 1 and 2) shows in general greater disagreement from the measured latent and sensible heat fluxes or the net radiation during the day than during the night, but these are marginal compared to the soil heat flux. For the maize field, the differences between measured and simulated soil heat flux during daytime are even larger than the residual. In night-time the soil heat flux is underestimated by up to 50 W m^{-2}, whereas the differences for all other fluxes are rather small. For the rye field, the curve of the differences between measured and simulated soil heat flux almost follows the curve of the residual. Hence REMO overestimates the soil heat flux during day and underestimates it during night. The sensible heat flux and the net radiation are overestimated by REMO in daytime and night-time.

SEWAB (Figures 3 and 4) shows uniform negative differences for all fluxes, which means that all components of the energy balance equation except for the net radiation are overestimated, with the latter underestimated in the simulation with the optimized parameters. Only in the case of the rye field during night, the soil heat flux is underestimated by exactly the amount of the positive

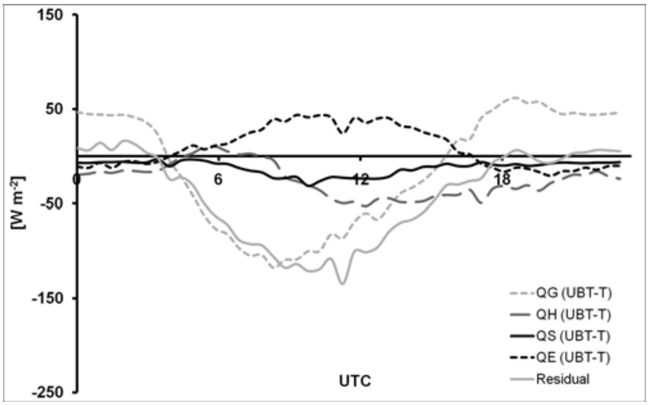

Figure 5: Differences between the energy fluxes simulated with TERRA (optimized parameters) for the maize field and the measured values, versus time of day. Also shown is the residual in the measured energy balance.

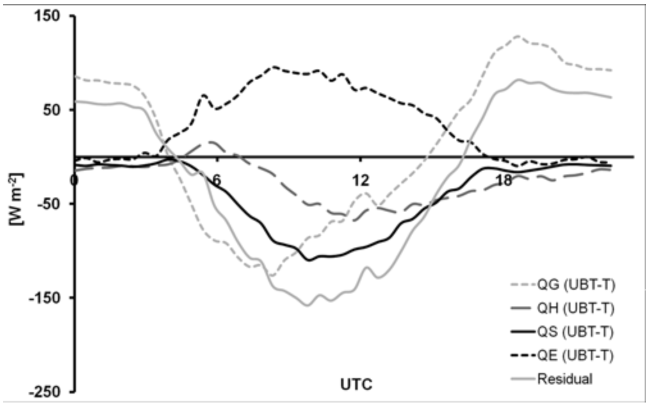

Figure 6: Differences between the energy fluxes simulated with TERRA (optimized parameters) for the rye field and the measured values, versus time of day. Also shown is the residual in the measured energy balance.

residual. The logical consequence of an underestimated net radiation would be underestimated turbulent fluxes, due to less available energy at the surface. SEWAB distributes the residual between the turbulent fluxes, which are consequently increased. The underestimation of the net radiation compensates for this increase of the turbulent fluxes due to the distribution of the residual and therefore results in a minimizing of the differences to the measured fluxes.

For both fields TERRA (Figures 5 and 6) shows, with optimized parameters, positive differences for the latent heat flux and negative differences for the other components of the energy balance equation, except for the soil heat flux, which is underestimated during night. The net radiation is underestimated for the rye field by approximately 100 Wm^{-2}, as well as the latent heat flux.

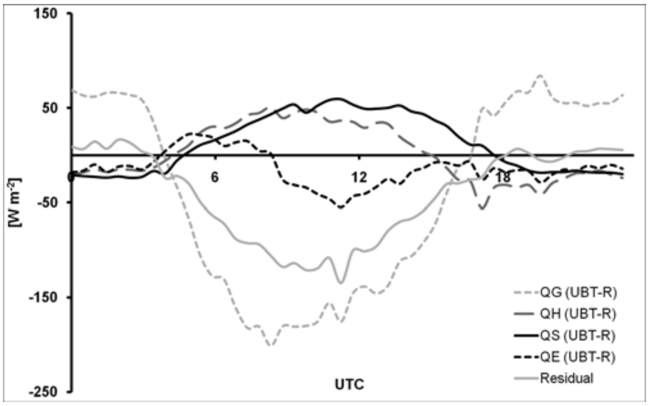

Figure 7: Differences between the energy fluxes simulated with REMO (realistic parameters) for the maize field and the measured values, versus time of day. Also shown is the residual in the measured energy balance.

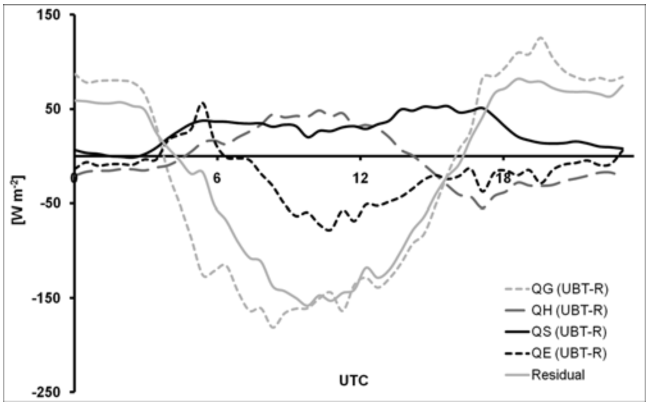

Figure 8: Differences between the energy fluxes simulated with REMO (realistic parameters) for the rye field and the measured values, versus time of day. Also shown is the residual in the measured energy balance.

Simulations with realistic parameters

As expected, all models produce greater deviations from the measurements when the simulations are carried out with the realistic parameters than when the simulations use the optimized parameters.

REMO (Figures 7 and 8) shows an enormous overestimation of the soil heat flux, which is even higher than the residual. As the net radiation is also overestimated, this results from a higher available energy. Around noon the curve of the soil heat flux shows the same behaviour as the curve of the residual.

The greatest differences between simulated and measured values are shown by SEWAB (Figures 9 and 10) with the realistic parameter set for the sensible heat flux, namely more than 100 W m^{-2} for the maize and more than 200 W m^{-2} for the rye field. The net radiation is overestimated for the maize field and underestimated for the rye field. For the rye field the deviations from the measurements are around zero during night for all fluxes

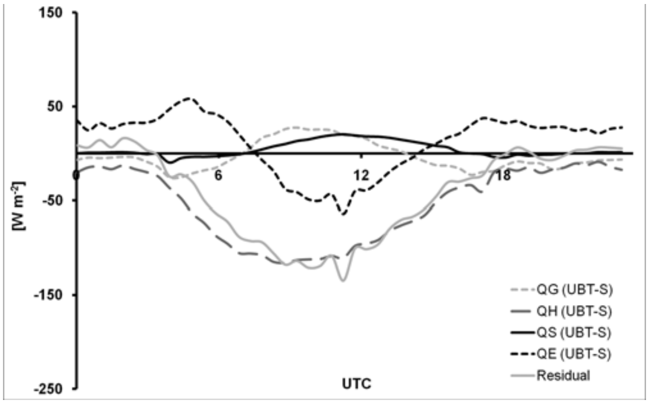

Figure 9: Differences between the energy fluxes simulated with SEWAB (realistic parameters) for the maize field and the measured values, versus time of day. Also shown is the residual in the measured energy balance.

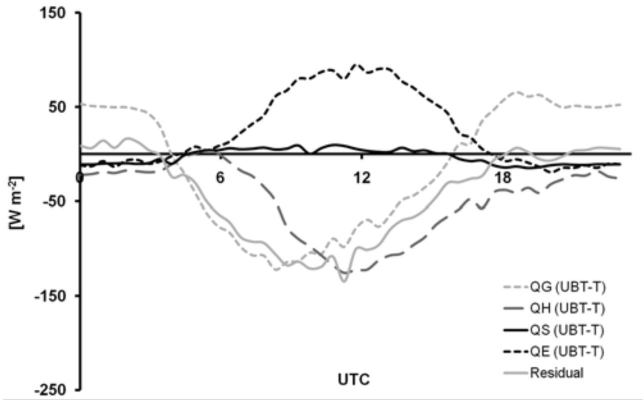

Figure 11: Differences between the energy fluxes simulated with TERRA (realistic parameters) for the maize field and the measured values, versus time of day. Also shown is the residual in the measured energy balance.

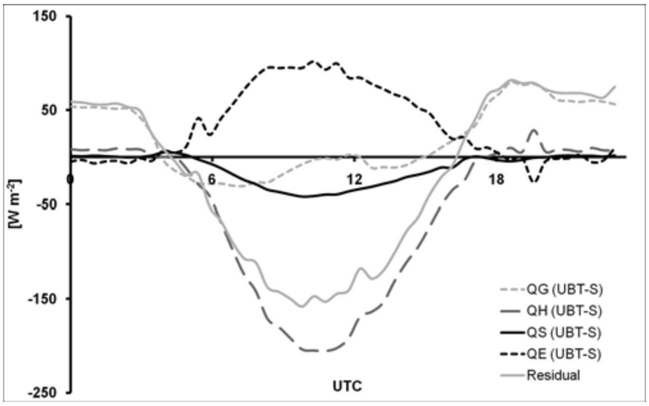

Figure 10: Differences between the energy fluxes simulated with SEWAB (realistic parameters) for the rye field and the measured values, versus time of day. Also shown is the residual in the measured energy balance.

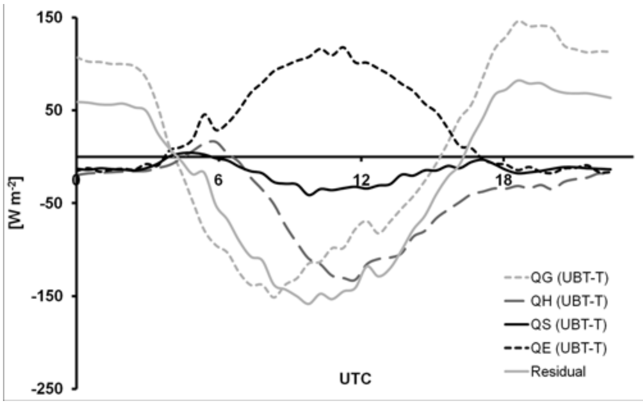

Figure 12: Differences between the energy fluxes simulated with TERRA (realistic parameters) for the rye field and the measured values, versus time of day. Also shown is the residual in the measured energy balance.

except for the soil heat flux, which is underestimated by the amount of the residual. During day time the soil heat flux is overestimated for the rye field and underestimated for the maize field, but the deviations from the measurements (50 W m^{-2}) are much smaller than with simulations using REMO and TERRA.

For the maize field, TERRA (Figures 11 and 12) overestimates the soil heat flux almost exactly by the amount of the residual, except for the night time, where the soil heat flux is underestimated, whereas all other fluxes are overestimated. The net radiation has, for both fields, the best correlation with the measurements. The soil heat flux is also overestimated for the rye field. At the beginning of the day the deviations from the measured soil heat flux are larger than the residual and later in the morning they become smaller, but around noon the curve of the residual and the curve of the differences between measured and simulated soil heat flux show the same distinctive characteristic. During night the soil heat flux is underestimated by more than 100 W m^{-2} but all other fluxes are overestimated, which is also the case for the maize field.

In most cases the differences between the turbulent fluxes simulated with TERRA and REMO and the measured values have the same magnitude for sensible and latent heat flux, but the opposite sign. For REMO and TERRA the sum of the simulated turbulent fluxes matches almost perfectly the measured ones (not shown). Consequently we concluded that the over- and under-estimation of both fluxes is due to an incorrect partitioning of the available energy within the model, and is independent from the way the energy balance is closed. Therefore the influence of the residual is clearly acting upon the soil heat flux. For SEWAB, any similarly incorrect partitioning is not as obvious.

Especially for the simulations with realistic parameters, it can be seen for REMO and TERRA that the plotted deviations of both simulated latent and sensible heat fluxes from the measured fluxes seem to be occasionally time shifted. In the models, variables which nor-

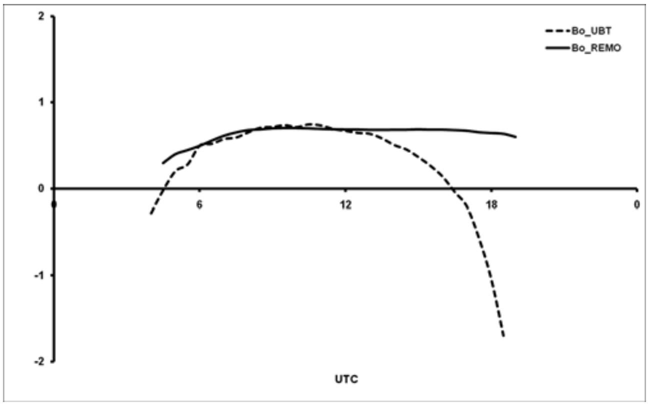

Figure 13: Bowen-ratio simulated with REMO (Bo_REMO) for the rye field with optimized parameters and the measured Bowen-ratio (Bo_UBT), versus time of day.

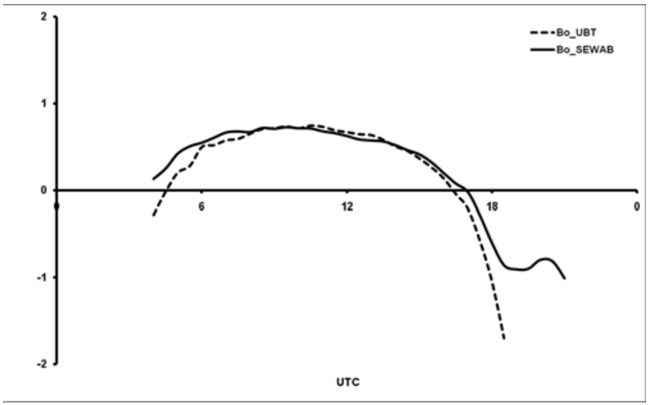

Figure 14: Bowen-ratio simulated with SEWAB (Bo_SEWAB) for the rye field with optimized parameters and the measured Bowen-ratio (Bo_UBT), versus time of day.

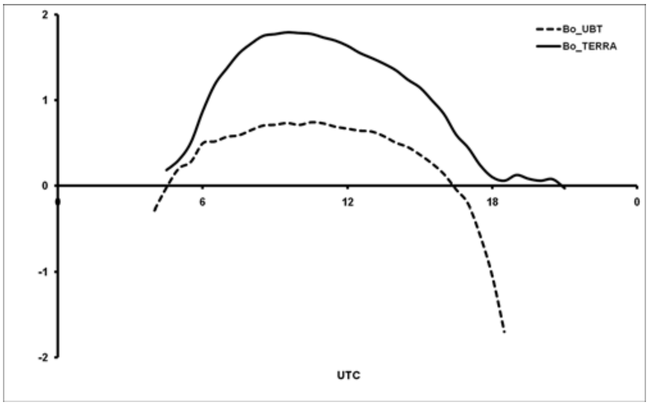

Figure 15: Bowen-ratio simulated with TERRA (Bo_TERA) for the rye field with optimized parameters and the measured Bowen-ratio (Bo_UBT), versus time of day.

mally change during the day are often set constant or calculated without taking into account their diurnal variation. Also an accurate parameterization of the soil, as is the case in SEWAB, cannot be found in REMO and TERRA.

REMO and TERRA are not able to simulate a negative Bowen ratio (Bo) during night (Figures 13 and 14), whereas the Bowen ratio given in SEWAB is closer to reality (Figure 15). The Bowen ratio is defined as the ratio of sensible heat flux to latent heat flux. It is positive when both fluxes have the same sign and negative when one flux is positive and the other negative. In stable conditions during night, the earth surface cools, so that the sensible heat flux is directed towards the surface and will therefore have a negative sign. The latent heat flux will be negative when the moisture flux is directed towards the earth surface, as is the case with dew formation. Stable conditions occur almost every night, whereas dew formation takes place only occasionally. Therefore the negative sign of the mean daily curves of the Bowen ratio is due to a negative sensible heat flux at night, which is not reproduced by TERRA and REMO. Consequently stable conditions at night are not well represented in these models.

It is obvious that the manner of balancing the soil heat flux in TERRA and REMO leads to an overestimation of this flux. Our version of the REMO model did not calculate the soil heat flux at all and therefore did not originally close the energy balance explicitly. The soil heat flux might not be of interest for the REMO model and therefore an overestimation might not be considered a disadvantage. In contrast SEWAB, which calculates the soil heat flux explicitly and closes the energy balance by an iteration of the surface temperature, distributes the residual uniformly over all energy fluxes.

As the equations for the net radiation and the soil heat flux had to be included in our version of REMO, these simulations need to be considered critically. However, for the net radiation we used as far as possible the equations already available in the model, and completed the equation in a manner similar to that used in SEWAB and TERRA. We presume that with our changes regarding the net radiation the REMO simulations were more realistic and therefore allow for better examinations of the residual's effect.

5 Conclusion

According to the current state of knowledge the nonclosure of the energy balance is due to an underestimation of the turbulent fluxes with eddy covariance measurements. Several studies have been conducted to examine the influence of uncertainties in the measurements of the net radiation (KOHSIEK et al., 2007) and the soil heat flux for the LITFASS-2003 experiment (LIEBETHAL et al., 2005; LIEBETHAL and FOKEN, 2007). As a conclusion the residual can be reduced by certain measures, but cannot be deleted. As the energy balance can be closed by measurements conducted in the desert (MAUDER et al., 2007b) it is obvious that the residual in the energy balance equations results from assumptions needed for the eddy-covariance technique that are not suitable for heterogenic terrain. Heterogeneity evokes processes that are not captured by the eddy-covariance technique, whereas they do not occur in homogeneous terrain such as in deserts, and can only be detected by using spatial measurements such as flights (MAUDER et al., 2007a; FOKEN, 2008).

Given this fact, an optimization of the model parameters which is too close to measured turbulent fluxes, without taking into account the residual, leads to a systematic error in the simulations. This can clearly be seen in the overestimation of the soil heat flux in REMO and TERRA. As the soil temperature influences many important processes, such as for example soil respiration (WANG et al., 2006) and consequently CO_2 emissions from soil (RUSTAD and FERNANDEZ, 1998), and water uptake by trees (MELLANDER et al., 2006), an accurate simulation of the soil heat flux is an essential requirement, especially for coupling with other models. For the usual purpose of the REMO and TERRA models the soil heat flux might not be of interest, as it was not originally calculated in the REMO code and not explicitly in TERRA. Also in terms of coupling with other models, the soil temperature might not be relevant in REMO and TERRA. However, especially for the prediction of extreme events, an accurate simulation of the temperature and the water availability in the atmosphere is essential. If the non-closure of the energy balance measured at the surface and the resulting under-estimation of the sensible and latent heat fluxes is not considered in the simulation, the model might not be able to predict such extreme events properly. Therefore all the components of the energy balance equation at the surface need to be simulated as exactly as possible, which implies an adequate partitioning of the residual over the fluxes.

In SEWAB, the iteration of the surface temperature seems to be an appropriate approach to close the energy balance, because the residual is partitioned upon all the fluxes. This also means that the simulated turbulent fluxes are higher than the measured fluxes and therefore more realistic. This is similar to the distributing of the residual according to the Bowen ratio (TWINE et al., 2000), which was also proposed by FOKEN (2008) as a first guess. Unfortunately the main reason for the energy balance closure problem are larger eddies which are not similar for temperature and moisture and other species (RUPPERT et al., 2006). It is still an open question how to distribute the residual over the sensible and latent heat flux, but simply partitioning it to the non-turbulent fluxes as done in TERRA, or not closing the energy balance at all as it was in our version of the REMO model, is obviously not appropriate. As long as there is no generally accepted method for distributing the residual upon the turbulent fluxes, introducing a term for the residual can be a temporary solution in modeling the energy balance at the Earth's surface. However, in order to simulate the sensible and latent heat flux as appropriately as possible, the residual needs to be distributed; otherwise the turbulent fluxes will be underestimated, as they are by eddy covariance techniques. One possibility would be to split the residual into one term that will be added to the sensible heat flux and another term that will be added to the latent heat flux according to the Bowen ratio (TWINE et al., 2000, FOKEN, 2008). Additionally the soil heat flux needs to be calculated explicitly instead of being used to close the energy balance. As models are developed and evaluated based on measurements, they also include the uncertainties related to the measurements. In that sense, achievements in research of the energy balance closure with eddy covariance measurements will also improve the models.

6 List of symbols

List of abbreviations

EVA-GRIPS Evaporation at grid/pixel scale
ISBA Interactions Soil Biosphere Atmosphere
LITFASS Lindenberg Inhomogeneous Terrain – Fluxes between Atmosphere and Surface: a long term study
MOL Meteorological Observatory Lindenberg
MOSCEM-UA Multiobjective Shuffled Complex Evolution Metropolis – University of Arizona
REMO Regionalmodell
SCE-UA Shuffled Complex Evolution – University of Arizona
SEWAB Surface Energy and Water Balance
SiSPAT Simple Soil-Plant-Atmosphere Transfer
SVAT Surface Vegetation Atmosphere Transfer
UBT University of Bayreuth
UTC Universal Time Coordonné

List of symbols

Latin symbols

a Albedo
a_B Albedo for bare soil
b Gradient of the logarithmic retention curve
C_E Dalton number
C_H Stanton number
C_{hn} Transport coefficient for temperature for neutral conditions
C_{mn} Transport coefficient for momentum for neutral conditions
c_p Specific heat of the air at constant pressure [J kg^{-1} K^{-1}]
c_{soil} Specific heat of the soil [J kg^{-1} K^{-1}]
C_W Cloud water content
E_P Potential evaporation
ET_B Evaporation of bare soil [mm s^{-1}]
ET_{Int} Evaporation of interception water [mm s^{-1}]
ET_V Transpiration [mm s^{-1}]
F_h Correction factor
f_{PAR} Fraction of photosynthetic active radiation

$K\downarrow$ Global radiation [W m^{-2}]
$K\uparrow$ Reflected shortwave radiation [W m^{-2}]
K_{netto} Net short wave radiation [W m^{-2}]
K_{sat} Saturated hydraulic conductivity [m s^{-1}]
$L\downarrow$ Incoming longwave radiation [W m^{-2}]
LAI Leaf area index [m^2 m^{-2}]
p Air pressure [hPa]
Q_E Latent heat flux [W m^{-2}]
Q_G Soil heat flux
Q_H Sensible heat flux [W m^{-2}]
$Q{*}_S$ Net radiation [W m^{-2}]
q Specific humidity [kg kg^{-1}]
r Relative humidity
R Residual [W m^{-2}]
Ri_B Bulk Richardson number
R_B Factor for calculation of humidity at surface
R_L Gas constant for dry air [J kg^{-1} K^{-1}]
r_a Atmospheric resistance [s m^{-1}]
r_s Stomatal resistance [s m^{-1}]
$r_{s,max}$ Maximal stomatal resistance [s m^{-1}]
$r_{s,min}$ Minimal stomatal resistance [s m^{-1}]
T temperature [K]
T_V Virtual temperature [K]
u Wind velocity [m s^{-1}]
V_{por} Pore volume [m^3]
z height [m]
z_0 Roughness length [m]
z_{0T} Roughness length for temperature [m]
z_c Canopy height [m]
z_r Root depth [m]

Greek symbols

Ψ Zenith angle of the sun
δ_I Fraction of leafs with interception water
δ_V Fraction of vegetation
ε Emissivity
η Volumetric water content [m^3 m^{-3}]
η_{fc} Field capacity [m^3 m^{-3}]
η_I Soil ice content
η_{sat} Volumetric water content at saturation [m^3 m^{-3}]
η_{WP} Volumetric water content at wilting point [m^3 m^{-3}]
κ von-Kármán-Constant
λ Heat of evaporation [J kg^{-1}]
λ_{soil} Soil heat conductivity cm^2 [s^{-1}]
Θ Potential temperature [K]
ρ Density of air [kg m^{-3}]
ρ_I Density of ice [kg m^{-3}]
ρ_{soil} Density of soil [kg m^{-3}
ρ_W Density of water [kg m^{-3}]
σ Stefan-Boltzmann-constant [W m^{-2} K^{-4}]
Ψ_{sat} Matrix potential at saturation [m]

Constants

$\sigma = 5{,}67\cdot10^{-8}$ W m^{-2} K^{-4}
$\rho = 1{,}223$ kg m^3
$c_p = 1004{,}7$ J kg^{-1} K^{-1}
$\rho_W = 1025$ kg m^{-3}

Acknowledgments

The authors acknowledge Klaus-Peter JOHNSEN und Sven HUNECKE for the calculation of the optimized parameters and Matthias Mauder for the calculation of the turbulence data of the sites A5 and A6. The LITFASS-2003 experiment was funded by the Federal Ministry of Education, Science, Research and Technology (DEKLIM, project EVA-GRIPS: BMBF 01LD0103).

References

AG BODEN, 1994: Bodenkundliche Kartieranleitung, 4. Auflage. – Hannover, 392 pp.

ALTMAN, P.L., D.S. DITTMER, 1966: Environmental Biology. – Federation of American Societies for Experimental Biology, Bethesda, Maryland, 694 pp.

AUBINET, M., A. GRELLE, A. IBROM, Ü. RANNIK, J. MONCRIEFF, T. FOKEN, A.S. KOWALSKI, P.H. MARTIN, P. BERBIGIER, C. BERNHOFER, R. CLEMENT, J. ELBERS, A. GRANIER, T. GRÜNWALD, K. MORGENSTERN, K. PILEGAARD, C. REBMANN, W. SNIJDERS, R. VALENTINI, T. VESALA, 2000: Estimates of the annual net carbon and water exchange of forests: The EUROFLUX methodology. – Advan. Ecol. Res. **30**, 113–175.

BEYRICH, F., H.-T. MENGELKAMP, 2006: Evaporation over a heterogeneous land surface: EVA_GRIPS and the LITFASS-2003 experiment – an overview. – Bound.-Layer Meteor. **121**, 5–32.

BEYRICH, F., J.-P. LEPS, M. MAUDER, U. BANGE, T. FOKEN, S. HUNEKE, H. LOHSE, A. LÜDI, W. M. L. MEIJNINGER, D. MIRONOV, U. WEISENSEE, P. ZITTEL, 2006: Area-averaged surface fluxes over the LITFASS region on eddy-covariance measurements. – Bound.-Layer Meteor. **121**, 33–65.

BRAUD, I., A.C. DANTAS-ANTONIO, M. VAUCLIN, J.L. THONY, P. RUELLE, 1995: A simple soil-plant-atmosphere transfer model (SiSPAT) development and field verification. – J. Hydrol. **166**, 213–250.

CLAPP, R.B., G.M. HORNBERGER, 1978: Empirical equations for some soil hydraulic properties. – Water Resour. Res. **14**, 601–604.

COSBY, B.J., G.M. HORNBERGER, R.B. CLAPP, T.R. GINN, 1984: A statistical exploration of the relationship of soil moisture characteristics to the physical properties of soil. – Water Resour. Res. **20**, 682–690.

CULF, A.D., T. FOKEN, J.H.C. GASH, 2004: The energy balance closure problem. – In: KABAT, P., M. CLAUSSEN, P.A. DIRMEYER, J.H. C. GASH, L.B. DE GUENNI, H. MEYBECK, R.A. PIELKE SR., C. VÖRÖSMARTY, R.W.A. HUTJES, S. LÜTKEMEIER (Eds.): Vegetation, water, humans and the climate. A new perspective on an interactive system. – Springer, Berlin, Heidelberg.

DUAN, Q., S. SOROOSHIAN, V.K. GUPTA, 1992: Effective and efficient global optimization for conceptual rainfall-runoff models. – Water Resour. Res. **28**, 1015–1031.

–-, —, —, 1994: Optimal use of the SCE-UA global optimization method for calibrating watershed models. – J. Hydrol. **158**, 265–284.

Dugas, W.A., L.J. Fritschen, J.W. Gay, A.A. Held, A.D. Matthias, D.C. Reicosky, P. Steduto, J.L. Steiner, 1991: Bowen ratio, eddy correlation and portable chamber measurements of sensible and latent heat flux over irrigated spring wheat. – Agric. Forest Meteor. **56**, 1–20.

Elagina, L. G., S.L. Zubkovskii, B.M. Kaprov, D.Y. Sokolov, 1973: Experimental investigations of the energy balance near the surface. – Trudy Glavny Geofiziceskij Observatorii **296**, 38–45.

Foken, T., 1990: Probleme bei der Bestimmung vertikaler turbulenter Feuchte-Transporte im Rahmen von ISLSCP-Experimenten (Ergebnisse von KUREX-88 und TARTEX-90). – Proceedings der Ersten Deutsch-Deutschen Klimatagung, Berlin, 8 pp.

—, 1998: Die scheinbar ungeschlossene Energiebilanz am Erdboden - eine Herausforderung an die Experimentelle Meteorologie. – Sitzungsberichte der Leibniz-Sozietät **24**, 131–150.

—, 2008: The energy balance closure problem – An overview. – Ecological Applications **18**, 1351–1367.

Foken, T., S. Oncley, 1995: Results of the workshop 'Instrumental and Methodical Problems of Land Surface Flux Measurements'. – Bull. Amer. Meteor. Soc. **76**, 1191–1193.

Foken, T., F. Wimmer, M. Mauder, C. Thomas, C. Liebethal, 2006: Some aspects of the energy balance closure problem. – Atmos. Chem. Phys. **6**, 4395–4402.

Foken, T., M. Mauder, C. Liebethal, F. Wimmer, J.-P. Leps F. Beyrich, S. Raasch, H.A.R. DeBruin, W.M.L. Meijninger, J. Bange, 2009: Energy balance closure for the LITFASS-2003 experiment. – Theor. Appl. Climatol., published online, DOI: 10.1007/s00704-009-0216-8.

Geiger, R., R.H., Aron, P. Rodhunter, 1995: The climate near the ground. – Friedr. Vieweg & Sohn Verlagsges. GmbH, Braunschweig, Wiesbaden, 528 pp.

Gottschalck, J.C., R.R. Gillies, T.N. Carlson, 2001: The simulation of canopy transpiration under doubled CO_2: The evidence and impact of feedbacks on transpiration in two 1-D soil-vegetation-atmosphere-transfer models. – Agric. Forest Meteor. **106**, 1–21.

Hartge, K.H., R. Horn, 1999: Einführung in die Bodenphysik. – Ferdinand Enke Verlag, Stuttgart, 304 pp.

Henderson-Sellers, A., A.J. Pitman, P.K. Love, P. Irannejad, T. Chen, 1995: The Project of Intercomparison of Land Surface Parameterisation Schemes (PILPS) Phases 2 and 3. – Bull. Amer. Meteor. Soc. **76**, 489–503.

Inagaki, A., M.O. Letzel, S. Raasch, M. Kanda, 2006: Impact of surface heterogeneity on energy balance: A study using LES. – J. Meteor. Soc. Japan **84**, 187–198.

Jacob, D., R. Podzun, 1997: Sensitivity Studies with the regional climate model REMO. – Meteor. Atmos. Phys. **63**, 119–129.

Johnsen, K.-P., S. Huneke, H.-T. Mengelkamp, 2006: Multi-objective calibration of the land surface scheme TERRA/LM using LITFASS-2003 data. – Hydrol. Earth Sys. Sci. **9**, 586–595.

Kanda, M., A. Inagaki, M.O. Letzel, S. Raasch, T. Watanabe, 2004: LES study of the energy imbalance problem with eddy covariance fluxes. – Bound.-Layer Meteor. **110**, 381–404.

Kohsiek, W., C. Liebethal, T. Foken, R. Vogt, S.P. Oncley, Ch. Bernhofer, H.A.R. DeBruin, 2007: The Energy Balance Experiment EBEX-2000. Part III: Behaviour and quality of the radiation measurements. – Bound.-Layer Meteor. **123**, 55–75.

Koitzsch, R., M. Dzingel, T. Foken, G. Mücket, 1988: Probleme der experimentellen Erfassung des Energieaustausches über Winterweizen. – Z. Meteorol. **38**, 150–155.

Larcher, W., 1994: Ökophysiologie der Pflanzen. – Verlag Eugen Ulmer GmbH & Co, Stuttgart, 394 pp.

Laubach, J., U. Teichmann, 1996: Measuring energy budget components by eddy correlation: data corrections and application over low vegetation. – Contribution to Atmospheric Physics **69**, 307–320.

Li, E.A., V.O. Shanholtz, E.W. Carson, 1976: Estimating saturated hydraulic conductivity and capillary potential at the wetting front. – Dep. of Agr. Eng., Va. Polytech. Inst. And State Univ., Blacksburg.

Liebethal, C., T. Foken, 2007: Evaluation of six parameterization approaches for the ground heat flux. – Theor. Appl. Climatol. **88**, 43–56.

Liebethal, C., B. Huwe, T. Foken, 2005: Sensitivity analysis for two ground heat flux calculation approaches. – Agric. Forest Meteor. **132**, 253–262.

Louis, J.F., 1979: A parametric model of vertical fluxes in the atmosphere. – Bound.-Layer Meteor. **17**, 187–202.

Louis, J. F., M. Tiedtke, J.F. Geleyn, 1982 : A short history of the PBL parametrization at ECMWF. – Workshop on Boundary Layer parametrization, Reading, ECMWF, 59–79.

Mauder, M., T. Foken, 2006: Impact of post-field data processing on eddy covariance flux estimates and energy balance closure. – Meteorol. Z. **15**, 597–609.

Mauder, M., C. Liebethal, M. Göckede, J.-P. Leps, F. Beyrich, T. Foken, 2006: Processing and quality control of flux data during LITFASS-2003. – Bound.-Layer Meteor. **121**, 67–88.

Mauder, M., R.L. Desjardins, J.I. MacPherson, 2007: Scale analysis of airborne flux measurements over heterogeneous terrain in a boreal ecosystem. – J. Geophys. Res. **112**, D13112, DOI: 10.1029/2006JD008133.

Mauder, M., O.O. Jegede, E.C. Okogbue, F. Wimmer, T. Foken, 2007a: Surface energy balance measurements at a tropical site in West Africa during the transition from dry to wet season. – Theor. Appl. Climatol. **89**, 171–183.

Mellander, P.E., M. Stahli, D. Gustafsson, K. Bishop, 2006: Modelling the effect of low soil temperatures on transpiration by Scots pine. – Hydrol. Proc. **20**, 1929–1944.

Mengelkamp, H.-T., K., Warrach, E., Raschke, 1999: SEWAB – a parameterization of the Surface Energy and Water Balance for atmospheric and hydrologic models. – Adv. Water Res. **23**, 165–175.

Mengelkamp, H.-T., J. Sutmoller, T. Zhao, 2002: Runoff simulation in the upper Oder catchment during the flooding event 1997 with a coupled atmospheric/ hydrological model. – Environmental change and Water Sustainability, Instituto Pirenaico de Ecología, Zaragoza, 141–150.

Monteith, J.L., 1976: Vegetation and the Atmosphere Vol.2: Case Studies. – Academic Press, 439 pp.

Noilhan, J., J.-F. Mahfouf, 1996: The ISBA land surface parameterisation scheme. – Global and Planetary Change **13**, 145–159.

NOILHAN, J., S. PLANTON, 1989: A simple parameterization of land surface processes for meteorological models. – Mon. Wea. Rev. **117**, 536–549.

NOVÁK, V., T. HURTALOVÁ, F. MATEJKA, 2005: Predicting the effects of soil water content and soil water potential on transpiration of maize. – Agricult. Water Manag. **76**, 211–223.

ORLENKO, L.R., S.I. LEGOTINA, 1973: Heat balance at the unterlying surface in the KENEKS-71 experiment. – Tr. Gl. Geofiz. Observ. **296**, 46–56.

RUPPERT, J., C. THOMAS, T. FOKEN, 2006: Scalar similarity for relaxed eddy accumulation methods. – Bound.-Layer Meteor. **120**, 39–63.

RUSTAD, L.E., I.J. FERNANDEZ, 1998: Experimental soil warming effects on CO2 and CH4 flux from a low elevation spruce-fir forest soil in Maine, USA. – Global Change Bio. **4**, 597–605.

SCHAAKE, J.C., 2003: Calibration of watershed Models, Introduction. – Water Sci. Application **6**, American Geophysical Union, (10/1029/006WS01), 1–7.

SCHEFFER, F., P. SCHACHTSCHABEL, 2002: Lehrbuch der Bodenkunde. - Spektrum Akademischer Verlag, Heidelberg, Berlin, 593 pp

SCHROEDER, D., 1992: Bodenkunde in Sticcworten, 5. Auflage. – Verlag Ferdinand Hirt AG in der Gebrüder Borntraeger Verlagsbuchhandlung, Berlin, Stuttgart, 175 pp.

SELLERS, P.J., 1985: Canopy reflectance, photosynthesis, and transpiration. – Int. J. Rem. Sens. **6**, 1335–1372.

STEINFELD, G., M.O. LETZEL, S. RAASCH, M. KANDA, A. INAGAKI, 2007: Spatial representativeness of single tower measurements and the imbalance problem with eddy-covariance fluxes: results of a large-eddy simulation study. – Bound.-Layer Meteor. **123**, 77–98.

STEPPELER, J., G. DOMS, U. SCHATTLER, H. W. BITZER, A. GASSMANN, U. DAMRATH, G. GREGORIC, 2003: Meso-gamma scale forecasts using the nonhydrostatic model LM. – Meteor. Atmos. Phys. **82**, 75–96.

TSVANG, L.R., M.M. FEDOROV, B.A. KADER, S.L. ZUBKOVSKII, T. FOKEN, S.H. RICHTER, J. ZELENY, 1991: Turbulent exchange over a surface with chessboard-type inhomogenities. – Bound.-Layer Meteor. **55**, 141–160.

TWINE, T.E., W.P. KUSTAS, J.M. NORMAN, D.R. COOK, P.R. HOUSER, T.P. MEYERS, J.H. PRUEGER, P.J. STARKS, M.L. WESELY, 2000: Correcting eddy-covariance flux underestimates over a grassland. – Agric. Forest Meteor. **103**, 279–300.

VRUGT, J A., H.V. GUPTA, L.A. BASTIDAS, W. BOUTEN, S. SOROOSHIAN, 2003: Effective and efficient algorithm for multiobjective optimization of hydrologic models. – Water Resour. Res. **39**, 1214, DOI: 10.1029/2002WR001746.

WANG, C.K., J.Y. YANG, Q.Z. ZHANG, 2006: Soil respiration in six temperate forests in China. – Global Change Bio. **12**, 2103–2114.

WARRACH, K., M. STIEGLITZ, H.-T. MENGELKAMP, E. RASCHKE, 2002: Advantages of a topographically controlled runoff simulation in a Soil-Vegetation-Atmosphere Transfer Model. – J. Hydrometeor. **3**, 131–148.

WILSON, K.B., A.H. GOLDSTEIN, E. FALGE, M. AUBINET, D. BALDOCCHI, P. BERBIGIER, C. BERNHOFER, R. CEULEMANS, H. DOLMAN, C. FIELD, A. GRELLE, B. LAW, T. MEYERS, J. MONCRIEFF, R. MONSON, W. OECHEL, J. TENHUNEN, R. VALENTINI, S. VERMA, 2002: Energy balance closure at FLUXNET sites. – Agric. Forest Meteor. **113**, 223–234.